EMBRY-RIDDLE
Aeronautical University™
SCHOLARLY COMMONS

Space Traffic Management Conference   2019 Progress through Collaboration

Feb 26th, 2:00 PM

Near Real Time Satellite Event Detection and Characterization with Remote Photoacoustic Signatures

Justin Spurbeck
University of Texas at Austin, jspurbeck@utexas.edu

Moriba K. Jah
University of Texas at Austin, moriba@utexas.edu

Follow this and additional works at: https://commons.erau.edu/stm

Part of the Astrodynamics Commons

Near Real Time Satellite Event Detection and Characterization with Remote Photoacoustic Signatures

Justin Spurbeck[1]
The University of Texas at Austin
Moriba K. Jah, Ph.D.[2]
The University of Texas at Austin

ABSTRACT

Active satellites frequently maneuver to mitigate conjunctions and maintain nominal mission orbits. With an ever-growing Resident Space Object (RSO) population, the need to detect and predict any changes in active RSO trajectories has become increasingly important. There is typically a lag on the order of hours to days from time of maneuver to unmodeled dynamic event detection depending on the magnitude of the delta-v. For uncooperative objects, this detection lag poses a threat to other satellites. Implementing an active photoacoustic signature change detection methodology to detect and predict unmodeled dynamic events would reduce the overall conjunction risk and provide a means for a near real time pulse of satellite events. If photometric data is collected at a sufficient rate, any changes in outgoing photon flux due to satellite body vibrations caused by on-board events can be detected. The analysis of high-rate light curve data in the photometric, frequency, and photoacoustic domains can thus help characterize the event and provide mission specific intelligence. This research also investigates the use of signal processing methods, primarily cross-correlation, to improve the satellite body minimum displacement detection threshold in the presence of noise induced by the chaotic atmosphere.

1. INTRODUCTION

One of the more challenging tasks for space domain operators and space debris mapping entities such as the Combined Space Operations Center (CSpOC), LeoLabs, and intelligence agencies is detecting space events in near real time. Typically, when an active spacecraft performs a maneuver, it can take on the order of hours for a delta-v of 1.0 m/s and sometimes days to detect a delta-v of 0.1-0.01 m/s. Assuming ideal optical tracking conditions, a large maneuver can be detected in at best fifteen minutes [1]. In addition to the detection lag, determining what type of on-board events occur is difficult, if not impossible, with current remote sensing techniques. If the trajectory of an RSO is not noticeably perturbed by a space event, it will likely go unnoticed. If there were a method to determine when and what kind of component-level operation takes place on an active satellite, it would provide critical insight into the its mission and allow for operational assessment along with improving response time to any uncooperative behavior. This paper will emphasize conclusions reached in [2] as well as extend its research in multiple areas relating to space object event detection, unique characterization, and operational parameter estimation via remote photoacoustic sensing.

2. PHOTOACOUSTIC SENSING & RSO EVENT CHARACTERIZATION

Assuming observability of the target RSO at event epoch, use of photoacoustic sensing would allow for near instantaneous detection of satellite events. We define remote photoacoustic sensing as the high-rate collection of photometric data because it can be played back acoustically. An on-board event such as a thruster fire can cause subtle vibrations in a satellite body. These vibrations reflect the outgoing photon flux in a manner proportional to the frequency of the vibrational mode and reflective properties of the satellite surfaces. Thus, a change in the frequency content contained in the high-rate photometric data can signal that an event has occurred. The detection lag is only limited by the speed of light and data processing workflow. Conversion from light to sound is made possible because the light leaving the satellite carries an equivalent information content that can be converted into an acoustic signal [3].

---

1 Graduate Student, Aerospace Engineering and Engineering Mechanics Department, Cockrell School of Engineering, The University of Texas at Austin, Austin, TX 78712.
2 Associate Professor, Aerospace Engineering and Engineering Mechanics Department, Cockrell School of Engineering, The University of Texas at Austin, Austin, TX 78712.

The use of sound may seem like a museum piece side effect of the photometric frequency content change detection methodology, but the perception of the data in the acoustic domain does yield important revelations. An example of where interpreting high-rate data as sound helped characterize an event is seen in the Voyager 1 plasma wave science mission [4]. The Voyager 1 spacecraft contains a plasma wave instrument that collected data on the vibrations caused by a pass-through of a cloud of dense, ionized gas while it was entering interstellar space. Conversion of this data to an acoustic signal by NASA mission scientists helped them gain insight into previously unrelated events. The acoustic perception of a rising tone in multiple ionized gas cloud passes helped infer an increasing density profile and thus a departure from our Solar System.

A more recent demonstration of this technique was reported from NASA's Mars InSight lander a few days after it touched down on the Martian surface. The spacecraft's seismometer and air pressure instruments detected vibrations caused by a 10-15 mph wind blowing across Mars' Elysium Planitia [5]. Acoustic playback yielded a "haunting low rumble" which was shifted up two octaves and sped up by a factor of 100 times to make it more audible for the human ear. The acoustic representation helped support claims consistent with a Martian dust devil observed from orbit near the landing area.

The direct application of photoacoustic sensing to Space Situational Awareness (SSA) is in deciphering what sort of event occurred on-board an active satellite. While analyzing high-rate photometric data in the frequency domain may allow for detection of an event such as a thruster fire, solar panel articulation, or scanning mirror activation, the frequency content alone may not be able to correlate the detection to what physical event actually occurred. The acoustic playback of the event should yield unique signatures that the human brain is very capable of detecting [6]. For instance, the vibration induced by a solar panel deployment and a scanning mirror on-board an imaging satellite likely have similar low frequency operational modes. Listening to the acoustic representation of these events should allow for the brain to differentiate between the articulation of the solar panel and event profile of a scanning mirror.

It should be noted that the end goal of photoacoustic sensing is not to simply add "humans in the loop" to constantly listen for active satellite events. This approach would be impractical for the scale of the SSA industry, although humans have been in the analysis loop for sonar detections in submarine warfare (e.g. determination between a depth charge, torpedo launch, or pod of whales). Once certain event profiles can be detected and correlated to a physical instrument activation with the help of the acoustic playback, it should be possible to begin training machine learning and pattern recognition algorithms to detect similar signals and associate them with certain RSOs. Those same algorithms could also begin to treat RSO event detections and nominal photometric profiles as biometric modalities that could be used to uniquely identify uncorrelated objects [7][8]. It may even become possible to predict events by correlating pre-event frequency and photoacoustic content with future satellite behavior.

3.   ACTIVE SATELLITE EVENT DETECTION

Efforts to detect a satellite event in near real time with 50 kHz photometric data as in [2] have not yielded an operator-confirmed event yet. Some anomalous transient burst detections are still under investigation. Until current optical systems are tweaked to allow for the desired space event detection, the authors have pursued other data sets. A final boost stage burn of the GSSAP and ANGELS satellite launch was inadvertently detected by an astrophotographer generating a time lapse of the night sky in July 2014 [9]. The final boost stage burn was very large, long, and at a low enough altitude to detect with a simple DSLR camera. Thus, this footage was a decent test candidate to determine if a representative acoustic signature of the thruster activation could be derived. The result of tracking, isolating, and enhancing the video to analyze the luminance time series of the thruster event is shown in Fig. 1.

To convert the RGB values to luminance, a standard derivation per the International Telecommunications Union was employed [10]. Normalization of the signal supports playback depending on the desired codec and audio player. As expected, the acoustic representation was not at all representative of an actual thruster fire event due to the video's low frame rate of 24 fps. The time lapse itself operated at one frame every three seconds, providing an effective acoustic source at only 8 Hz. The shift and scale methods used by the Mars InSight lander team were useless due to the limited length of data. In some video production and visual effects suites, an interpolation method can used to estimate pixel motion within a frame. The motion estimation can then be used to generate an intermediate frame or average of the two neighboring frames. While this method works great for non-flickering objects, applying interpolation to this footage would effectively be generating noise in between each frame as the true frequency content of the thruster event would remain unknown.

To prove that the video to sound process is a realistic conversion, the method was implemented on high-rate ground test footage of a Bloodhound SSC rocket [11]. The 4,000 fps frame rate is much more suitable for a proof of concept as compared to the 8 Hz source from before even though it contains only one second of real time playback. As before, a time-series of luminance values were generated from various regions of the source frames as shown in Fig. 2. The time series of this video produces a much more realistic acoustic representation of the actual sound and stands as proof of concept for the light to sound conversion of an Earth-orbiting satellite firing its thrusters. The true sound of a Bloodhound SSC can be heard as in [12] for comparison.
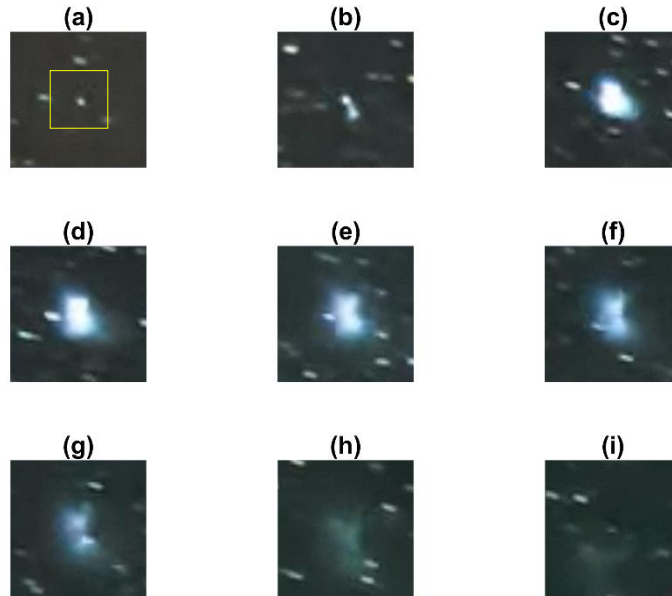

Fig. 1. Nine frames taken from [9] during final boost stage maneuver. The footage has been tracked, stabilized, and enhanced via sharpening and contrast adjustments. *(a)* Yellow outline showing the area of interest and pixels used in producing the luminance time-series. *(b)* Ignition and initial plume. *(c)* Growing plume. *(d)* Continuous plume. *(e)-(h)* Plume starts to fade. *(i)* Final stage burn mostly complete or plume unobservable.
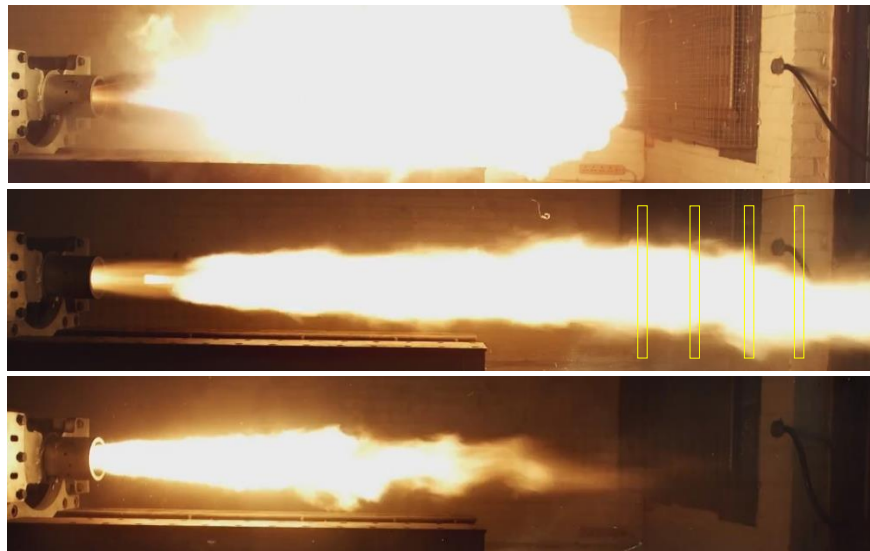

Fig. 2. High-speed (4,000 fps) video of a Bloodhound SSC rocket ground test used for optical-to-sound proof of concept [10]. The acoustic conversion yields a very nice thruster dissipation sound along with a higher pitched nominal operation. *(Top)* Thruster plume a few milliseconds post-ignition. *(Middle)* Nominal thrust. Yellow rectangles show the various pixel areas used in deriving the luminance values for acoustic signal generation. *(Bottom)* Thrust down and plume dissipation.

Selection of which pixels to use to represent the true "flicker" of the plume should be done with caution. Depending on the video processing algorithm's formulation, selecting all available pixels can result in a frequency averaging effect which seems to decrease the realness of the audio. A human interprets audio as pressure waves propagating through the air, and the tail of the Bloodhound SSC plume is the most turbulent section. Most of the tested luminance time series were generated from vertical slices of the plume's tail as seen in Fig. 2, but larger sections produced useable results as well. Due to camera proximity, the quality and uniqueness of the pixels used in the Bloodhound footage were more suitable for audio generation compared to the highly cropped pixels in the GSSAP-ANGELS data.

Another challenge encountered while collecting real photoacoustic data has been the strong noise floor present in the measurements that masks potential satellite operational signatures. Due to the complex processes that exist in Earth's atmosphere, the incoming light reflected from any RSO will have a degree of randomness to it. Optical equipment sensitivity also plays a role in the additive noise. It has been shown in [2] that satellite vibrations with body displacement values down to 3.46 cm can be detected based on an atmospheric noise assumption of a zero-mean Gaussian apparent magnitude with 0.04 standard deviation. The simulated detections are reproduced via spectrogram in Fig. 3 for reference.
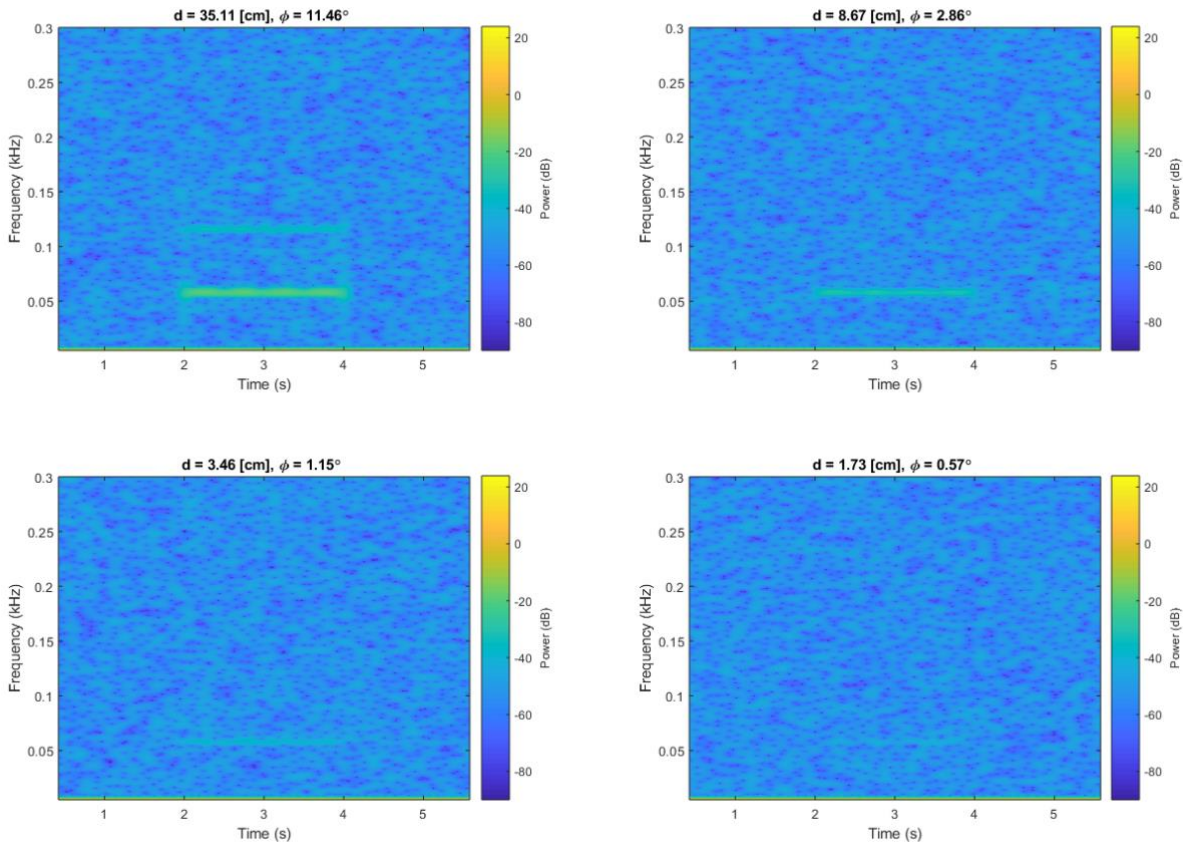

Fig. 3 – Simulation results from [2] showing that as the satellite body displacement values caused by an on-board event such as a thruster fire decrease, the 58 Hz signal detection becomes more difficult. The value d corresponds to the peak surface deflection value (end of solar panel or edge of box model). The angle ϕ is the maximum degree of rotation the surface unit vector experiences in the satellite vibration model discussed in Eq. (2). A 2N harmonic shows up in *(top left)* due to a large ϕ value.

Acoustic playback of the Fig. 3 simulations resulted in tonal "hums" as opposed to a more chaotic thruster fire sound like the Bloodhound test since the surface vibration is producing the acoustic signal, not direct observations of an exhaust plume. The simulation used a box-wing satellite model and assumed a simplistic box-shear or clamped cantilever vibration mode per surface as described in Eq (2) to accomplish the surface unit normal vector oscillation.

$$\phi = \phi_{max} \sin(\omega[t - t_{burn}]) \tag{1}$$

$$\hat{u}_{surface}(t) = R_n(\phi)\hat{u}_{nominal}(t) \tag{2}$$

The ϕ_{max} parameter is the desired peak deflection angle, ω is the chosen event forcing frequency, $R_n(\phi)$ is the rotation matrix about the appropriate axis, and the two $\hat{u}$ surface unit vectors are the nominal pointing and vibration-perturbed values respectively. In the future, a more realistic area deformation macro model should be used to better represent a satellite's vibrational modes. For the low displacement modes, the differences are likely close to negligible or on the same order of magnitude. The 58 Hz source signal was chosen somewhat arbitrarily but mainly to avoid low frequency power observed in experimental data. It appears that activate satellite vibration modes can live in the 3-12 Hz range based on on-orbit test data, but it will vary depending on mission requirements [13]. Tribal knowledge gathered from industry experience points towards some active modes being above 50 Hz. In general, the highest displacements will come from the lowest mode frequencies, so the 58 Hz value is likely a bit high. The conclusions remain the same as the included simulations could be re-run with the lower frequency to produce a shifted detection value. A Cook-Torrance reflectance model was employed per [14] for each box-wing surface.
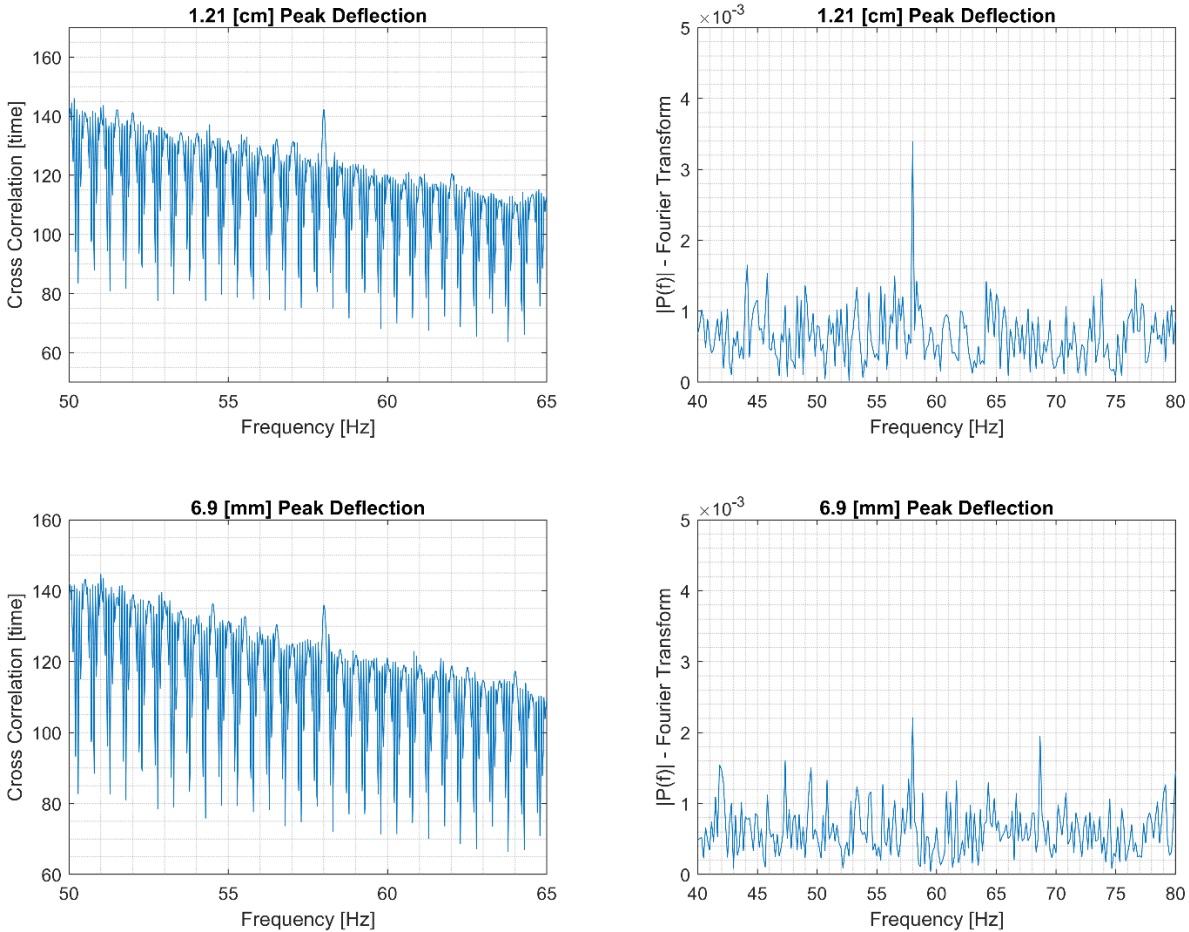

Fig. 4. *(Top-left)* Results of the cross-correlation method applied to simulated data showing an event detection at 58 Hz, SNR was -22.69 dB. *(Top-right)* Same event detected at 58 Hz via traditional Fast Fourier Transform. *(Bottom-left)* Weaker signal detected with a lower satellite body displacement corresponding to a 6.9 [mm] peak displacement, SNR was -27.55 dB. *(Bottom-right)* The FFT struggles to produces a unique, distinguishable signal due to the minute vibration amplitude simulated in this case.

To improve upon the 3.46 cm minimum detectable displacement value, a standard signal processing method known as cross-correlation was implemented. The algorithm implemented scanned all frequency bands in small increments to determine which frequency produced the highest correlation with the simulated data. As shown in Fig. 4, the cross-correlation technique was indeed able to pull a signal from the noise floor that the standard spectrogram analysis could not. The spectrogram likely isn't the best domain to visualize a detection so the traditional Fast Fourier Transform (FFT) was also employed to compare from a single-sided amplitude spectrum perspective. Before, the minimum detectable relative displacement value was 3.46 cm and solar panel end tip deflection was 7.75 cm. With cross-correlation and traditional FFT techniques, the values were reduced to 6.9 mm and 1.55 cm respectively, thus improving the ability to detect minute satellite body vibrations. Using a best-case atmospheric noise standard deviation

of 0.03 for apparent magnitude allowed detection down to a minimal 5.2 mm deflection, again at 58 Hz. It seems like cross-correlation performs better than a traditional FFT for the 6.9 mm deflection case. The base Fourier Transform and cross-correlation formulations are quite similar in nature convolution-wise, so why one cannot distinguish the signal as well as the other is difficult to determine.

As seen in the results, the ability to detect space events with remote photoacoustic methods is sensitive to atmospheric noise. It is uncommon to see Gaussian distributions with standard deviations as high as 0.1-0.3, but it does occur. All cases in this research assumed a 0.04 standard deviation unless explicitly stated. Standard deviations of 0.03-0.05 appear to be the best case for real optical data in industry [15]. The zero-mean, 0.04 standard deviation distribution was chosen to be not overly optimistic yet still in the highly precise optics and data analysis arena. The algorithmic nuances of reference signal length, shift interval, frequency interval as well as physical parameters such as the burn duration, satellite shape, and material properties will also affect the ability to pull any event signals from the atmospheric noise. A five second burn duration was used in producing the Fig. 4 analysis. The signal to noise ratios (SNR) for each case in Fig. 4 were -22.69 dB and -27.55 dB respectively.

Applying the cross-correlation method in time and frequency domains to real photoacoustic data collected in [2] around the time of known satellite maneuvers in geosynchronous Earth orbit (GEO) has not uncovered any hidden signals yet. This suggests we still have work to do in our optical detection sensitivity improvement and noise reduction efforts.

4. MANEUVER ESTIMATION & SPACECRAFT OPERATIONAL ASSESSMENT

Assuming a precise time stamp of thruster on and off times can be obtained through the photoacoustic change detection methodology discussed in the prior section, a whole host of spacecraft parameters can be estimated. It's been shown in [2] that if maneuver duration can accurately be observed to within a few tenths of a second, the delta-v magnitude, direction, and maneuver type can best estimated as soon as an RSO's state can be resolved with active measurements post maneuver. Using an Extended Kalman Filter with a 4.0 km a priori uncertainty for each position component, a 1.0 km offset for the initial state position guess, and a station tasking scheme involving two sensors and a realistic measurement gap showed that it's plausible to resolve a state within five minutes of thruster off time using the innovations covariance as a first order indicator of filter convergence. This simulation shows that when experimentally proven, photoacoustic sensing makes real time spacecraft event detection and near real time operational assessment and RSO parameter estimation possible.

Using the now known direct timestamps of the maneuver impulse allows us to apply conservation of orbital momentum and energy to solve for more mission specific spacecraft parameters useful in characterizing and assessing active satellites. For instance, if an a priori satellite mass estimate is known, the satellite's thruster mass flow rate, fuel consumption, specific impulse, and exhaust velocity can be estimated as follows by solving either of Eq. (3) or (7) for mass flow rate [2]. Using conservation of angular momentum,

$$m_i \bar{r}_i \times \bar{v}_i + \int_{t_i}^{t_f} \bar{r}(t) \times \left[\frac{-\Delta v \, \dot{m}}{\ln\left[1 - \frac{\dot{m}\Delta t}{m_i}\right]} \, \hat{a}(t)_{thrust} \right] dt = (m_i - \dot{m}\Delta t) \, \bar{r}_f \times \bar{v}_f \tag{3}$$

where all parameters are known quantities from the RSO state, delta-v, and a priori mass estimate. We continue by using conservation of orbital energy and solving analytically for the acceleration due to thrust,

$$F_{thrust} = I_{sp} g_0 \dot{m} = m a_{thrust} \tag{4}$$

$$\frac{\Delta m}{m_i} = 1 - e^{-\Delta v / I_{sp} g_0} \tag{5}$$

$$\bar{a}_{thrust}(t) = \frac{-\Delta v \, \dot{m}}{(m_i - \dot{m}t) \ln\left[1 - \frac{\dot{m}\Delta t}{m_i}\right]} \, \hat{a}(t)_{thrust} \tag{6}$$

$$\frac{1}{2}\,m_i\bar{v}_i^2 \;-\; m_i[U_E(\bar{r}_i)] \;+\; \int_{t_i}^{t_f}\left[\frac{-\Delta v\,\dot{m}}{ln\left[1-\frac{\dot{m}\Delta t}{m_i}\right]}\,\hat{a}(t)_{thrust}\right]\cdot \bar{v}(t)\,dt \;=\; (m_i-\dot{m}\Delta t)\left[\frac{1}{2}\,\bar{v}_f^2 - [U_E(\bar{r}_f)]\right] \qquad (7)$$

where U_E is the gravitational potential given by any of the standard spherical harmonics formulations. The work term can be vectorized using the delta-v direction. The position, velocity, and acceleration terms as functions of time are known due to a constrained delta-v magnitude and direction. The acceleration function can be a polynomial fit or left analytical as in Eq. (3) and (7). This yields another solvable equation across the work-energy terms. With a known mass flow rate and impulse duration, the amount of fuel consumed through a maneuver can also be calculated. The standard rocket equation allows us to solve for specific impulse and later exhaust velocity if desired. If Eq. (3) and Eq. (7) were linearly independent with respect to the mass term, this methodology would allow for spacecraft mass estimation and not require an a priori mass estimate. As shown in [2], applying this method to a known spacecraft trajectory in GEO with operator confirmed values yielded the results in Table 1. All simulations used a high-fidelity force model including a 20x20 EGM-96 gravity model, luni-solar perturbations, exponential drag, and an area-averaged solar radiation pressure model. A complex Earth model using an FK5 precession, nutation, and polar motion correction was also implemented. The only assumptions made were that a ballistic coefficient and equivalent solar coefficient-area-mass combination were estimated via observations made on the object prior to a maneuver like how CSpOC provides these values in a Conjunction Data Message (CDM).

Table 1. Estimation results for the Optus spacecraft operational parameters

Parameter	Accuracy	Notes
Delta-v magnitude	Within 0.51% of true value	-
Delta-v direction	Within 1.72 deg of true pointing vector	-
Maneuver type	SMA (a) lowered, Incl. (i) & Ecc. (e) increased	N-S station keeping
Mass flow rate ($\dot{m}$)	Within <2% of truth	-
Specific impulse (I_{sp})	Within <3% of truth	-
Fuel consumed (Δm)	Within <1% of truth	-
Exhaust velocity (v_e)	Agrees with generic values	True value not provided

5. FUTURE WORK

To allow for an experimental detection of a propulsive event on-orbit, we must continue to refine the optical systems at our disposal and optimize the signal to noise ratio in any collected data. Working closely with willing satellite operators to plan observable maneuvers will also be of high importance. It would be good to collect on a large maintenance maneuver as opposed to a small collision avoidance burn to increase our chances at detection. It would also be interesting to trend the atmospheric noise distribution standard deviation versus the minimum detectable satellite surface displacement threshold to help predict what sort of SNR is needed for realistic on-orbit surface displacements. Also, if it were possible to maintain linear independence with respect to mass in the conservation of orbital energy and momentum equations, standalone mass estimation would become possible. It turns out linear independence is not possible since each of those quantities are derived from Newton's Law of Universal Gravitation, so this method may need to be coupled with data fusion methodologies as in [16] to allow for Table 1 mass related parameter estimation. Finally, expanding the capabilities of the optical data to sound conversion workflow through various known techniques as in [17] would be useful to improve realism of photoacoustic signature playback.

6. CONCLUSIONS

This work summarized prior results proposed in [2] that allow for near real time space event detection, satellite operational assessment, and unique RSO identification. It was shown that with known maneuver start and end epochs thanks to photoacoustic sensing, a first order approximation of the burn duration, forcing frequency, delta-v magnitude, direction, and maneuver type could be accurately estimated within five minutes of thruster off-time. Also, if an a priori estimate of mass is known, it is possible to estimate thruster mass flow rate, specific impulse, exhaust velocity, and fuel consumed by a maneuver via impulse-momentum and work-energy methods in the same time frame. This sort of near real time estimation scheme increases general SSA capabilities and supports operational risk reduction by greatly shrinking the maneuver detection lag.

This research also extended the space event detection methodology by implementing more precise signal identification routines. Cross-correlation and a traditional FFT were used to help pull event signals from the noise floor produced by the chaotic atmosphere. It was shown that the minimum satellite body surface displacement threshold could be reduced from 3.46 cm to 6.9 mm for a 5.0 second duration maneuver on a satellite in low Earth orbit with cross-correlation. Also, a technique was presented to extract photoacoustic signatures from standard video given a sufficient frame rate. Finally, it was demonstrated that a realistic acoustic representation can be generated from a 4,000 fps video of a Bloodhound SSC rocket ground test – opening the door for real, on-orbit remote photoacoustic signature detections of propulsive events given a proper collection rate, observability, and SNR.

7.   ACKNOWLEDGEMENTS

8.   REFERENCES

[1]   Aaron, B.S., "Geosynchronous satellite maneuver detection and orbit recovery using ground based optical tracking." Masters Thesis, Massachusetts Institute of Technology, 2006.

[2]   Spurbeck, J., Jah, M., Kucharski, D., Bennet, J., Webb, J. "Satellite Characterization, Classification, and Operational Assessment Via the Exploitation of Remote Photoacoustic Signatures." *Advanced Maui Optical and Space Surveillance Technologies Conference*, Maui, Hawaii, 2018.

[3]   Slater, D., Ridenoure, R., Klumpar, D., Carrico, J., and Jah, M. "Light to Sound: The Remote Acoustic Sensing Satellite (RASSat)." *30th Annual AIAA/USU Conference on Small Satellites*, Logan, Utah, 2016.

[4]   Gurnett, D.A., Kurth, W.S., Burlaga, L.F., and Ness, N.F. "In Situ Observations of Interstellar Plasma with Voyager 1," *Science*, vol 341, pp. 1489-1492. 12 September 2013, DOI: 10.1126/science.1241681.

[5]   NASA/JPL-Caltech/CNES/IPGP/Imperial College/Cornell, "NASA InSight Lander 'Hears' Martian Winds." December 7, 2018. Retrieved from <https://mars.nasa.gov/news/8397/nasa-insight-lander-hears-martian-winds/?site=insight>

[6]   Dennis, J., Yu, Q., Tang, H., Tran, H., and Li, H. "Temporal coding of local spectrogram features for robust sound recognition," *Acoustics, Speech and Signal Processing (ICASSP), 2013 IEEE International Conference*, 26-31 May 2013 DOI: 10.1109/ICASSP.2013.6637759.

[7]   Jain, A., Ross, A., and Prabhakar, S. "An Introduction to Biometric Recognition," *IEEE Transactions on Circuits and Systems for Video Technology*, vol 14, No. 1, January 2004.

[8]   Adeoye, O. "A Survey of Emerging Biometric Technologies," *International Journal of Computer Applications*, vol. 9, No. 10, November 2010.

[9]   Halverson, R. "Final Boost Stage of GSSAP and ANGELS satellites." Dakotalapse. 28 July 2014. Retrieved from <http://dakotalapse.com/2015/01/final-boost-stage-4k-uhd/>

[10]   International Telecommunication Union, "Parameter values for the HDTV standards for production and international programme exchange." Rec. ITU-R BT.709-6. June 2015. Retrieved from <https://www.itu.int/dms_pubrec/itu-r/rec/bt/R-REC-BT.709-6-201506-I!!PDF-E.pdf>

[11]   iX Cameras, "Bloodhound SSC rocket test 2,000 fps and 4,000 fps mono and color." 15 February 2017. Retrieved from <https://www.ix-cameras.com/ballistics_high-speed_video_gallery/rockets_high-speed_video.php>

[12]   Bloodhound SSC, "Bloodhound's new 1,000mph Hybrid Rocket – Tested." 12 December 2014. Referenced at 1:55. Retrieved from <https://www.youtube.com/watch?v=Tk67Z_mai_k>

[13] Haugse, E., Juengst, C., Salus, W., and Lollock, J. "On orbit system identification," *37th Structures, Structural Dynamics and Materials Conference and Exhibit,* 15-17 April 1996, Salt Lake City, Utah. Technical Papers. Pt. 4 (A96-26801 06-39), AIAA p 2398-2407.

[14] Wetterer, C.J., and Jah, M. "Attitude Estimation from Light Curves," *Journal of Guidance, Control, and Dynamics*, vol. 32, No. 5, 2009, pp. 1648-1651.

[15] Personal communications with Dr. Tamara Payne of Applied Optimization, Inc. regarding how to model atmospheric effects on apparent visual magnitude.

[16] Mallik, V., Jah, M.K. Reconciling space object observed and solar pressure albedo-areas via astrometric and photometric data fusion. Adv. Space Res. (2018), https://doi.org/10.1016/j.asr.2018.08.005.

[17] Davis, A., et. al., "The Visual Microphone: Passive Recovery of Sound from Video," *ACM Transactions on Graphics,* vol. 33, Issue 4, Article No. 79.